

Supplementary Material

Supplementary Figures

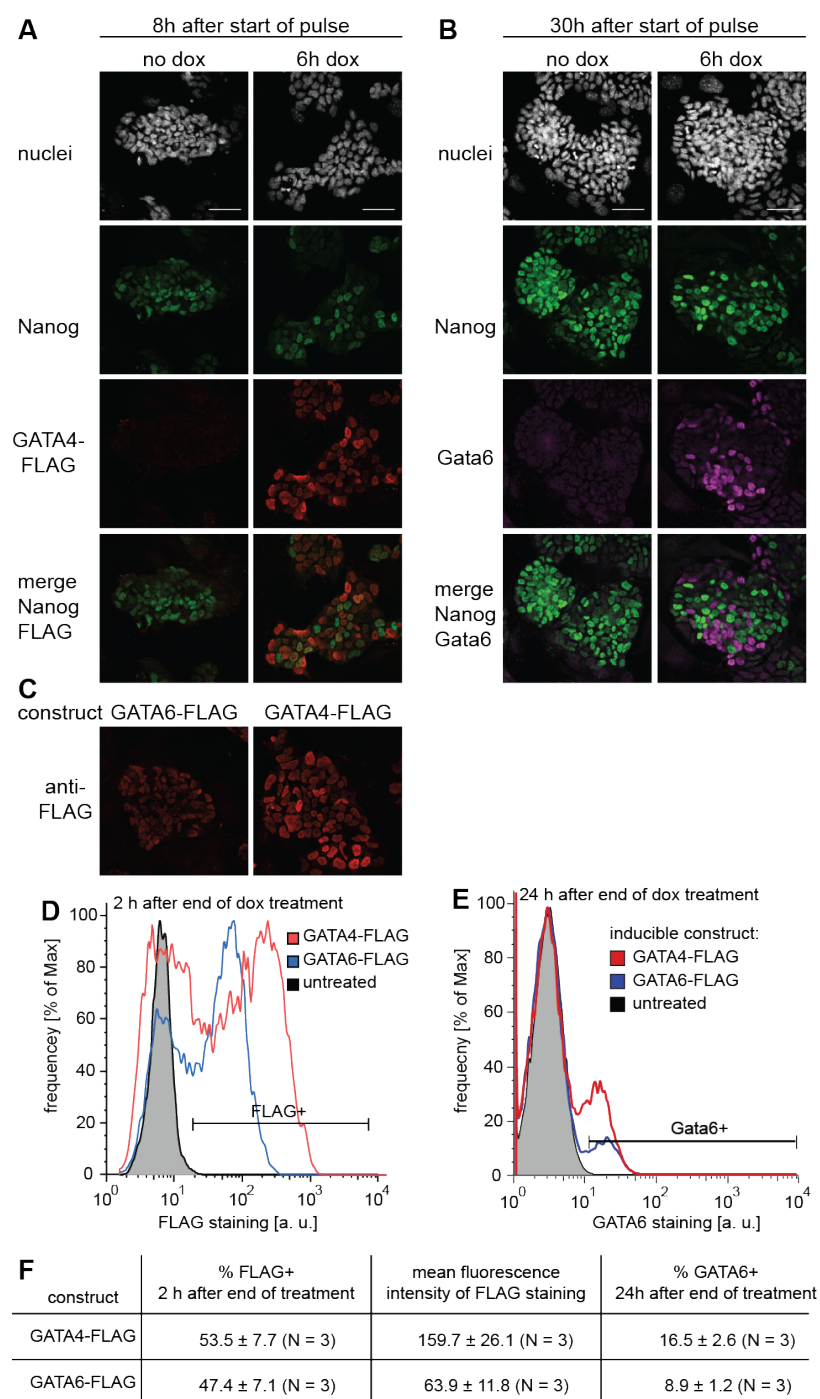


Fig. S1: Inducible GATA4-FLAG reaches higher expression levels and triggers PrE-like differentiation in a larger proportion of cells compared to GATA6-FLAG.

A, B Immunostaining of ES cells carrying a doxycycline-inducible GATA4-FLAG transgene 2 h (**A**) or 24 h (**B**) after 6 h of treatment with doxycycline. Untreated controls are on the left. Exogenous GATA4-FLAG is co-expressed with Nanog shortly after the treatment, but degraded one day later. Endogenous GATA6 is expressed one day after the treatment in a mutually exclusive pattern with Nanog. Scale bar, 50 μm . **C, D** Comparison of GATA6-FLAG and GATA4-FLAG transgene induction efficiency. Cells were immunostained for FLAG 2 h after a 6 h doxycycline pulse and analysed by confocal microscopy (**C**) or flow cytometry (**D**). The percentage of expressing cells is comparable between the two constructs, but GATA4-FLAG is expressed at higher levels in individual cells. One representative clone shown. **E** Flow cytometric analysis of cells immunostained for GATA6 24 h after transient expression of GATA4-FLAG (red) or GATA6-FLAG (blue). Inducible GATA4-FLAG expression triggers endogenous GATA6 expression in a larger proportion of cells compared to inducible GATA6-FLAG expression. One representative clone shown. **F** Quantitation of results from **D** and **E**; numbers state mean and standard deviation from three independent clones.

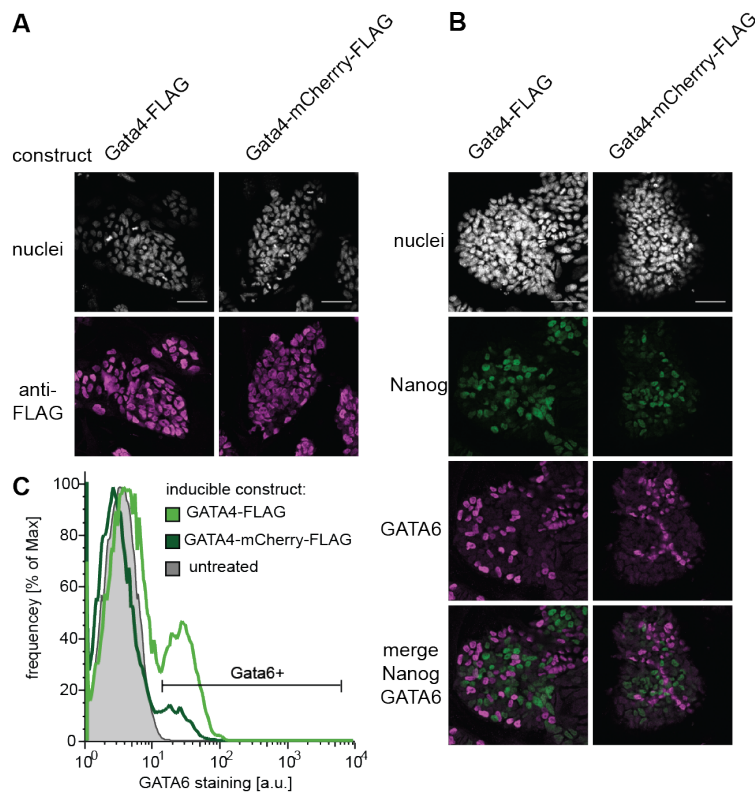


Fig. S2: Transient expression of GATA4-mCherry-FLAG can induce endogenous GATA6 expression.

A Immunostaining for FLAG in cells expressing GATA4-FLAG (left) or GATA4-mCherry-FLAG (right) following 6 h of doxycycline treatment. Both inducible proteins are expressed in a comparable proportion of cells, but FLAG staining intensity is lower for the mCherry-tagged protein, suggesting lower expression levels in individual cells. **B** Immunostaining for Nanog and GATA6 of cells carrying a doxycycline-inducible GATA4-FLAG (left) or GATA4-mCherry-FLAG (right) transgene 24 h after a 6 h treatment with doxycycline. Scale bars in **A**, **B**, 50 μm . **C** Flow cytometric analysis of cells treated as in **B** stained for GATA6 expression. GATA6 expression levels do not depend on the inducible protein used, but GATA4-mCherry-FLAG induces expression of endogenous GATA6 in a smaller proportion of cells than GATA4-FLAG, possibly as a consequence of lower GATA4-mCherry expression levels in individual cells.

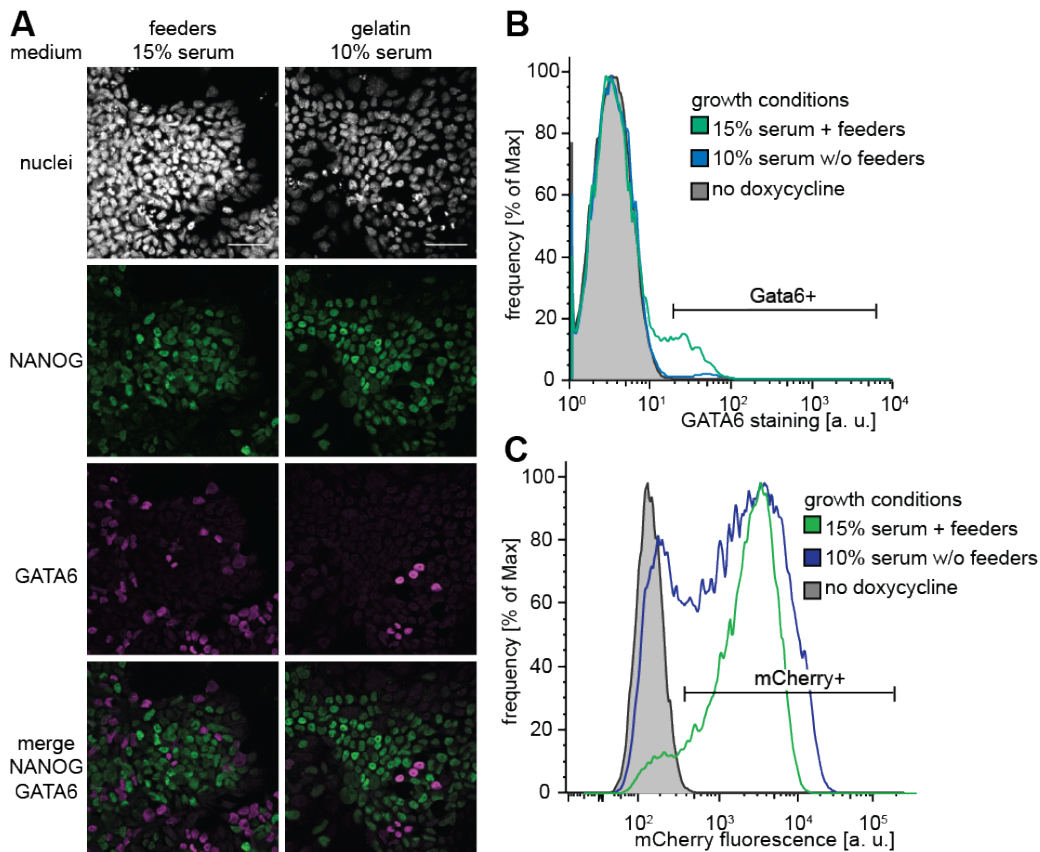


Fig. S3: Removal of feeders and reduction of serum levels reduces the accessibility of the PrE-like differentiation program.

A Immunostaining of cells carrying an inducible GATA4-mCherry transgene cultured on feeder cells in the presence of 15% serum (left) or in the absence of feeders in 10% serum (right) 24 h after a 6 h doxycycline pulse. Scale bar, 50 μm . **B** Flow cytometric analysis of cells treated as in **A** and stained for GATA6. The proportion of GATA6-positive cells is severely reduced in the absence of feeders and lowered serum concentrations. **C** Flow cytometric analysis of GATA4-mCherry expression in cells treated as in **A** 2h after the end of the doxycycline treatment. Both conditions give robust expression of the inducible GATA4-mCherry protein.

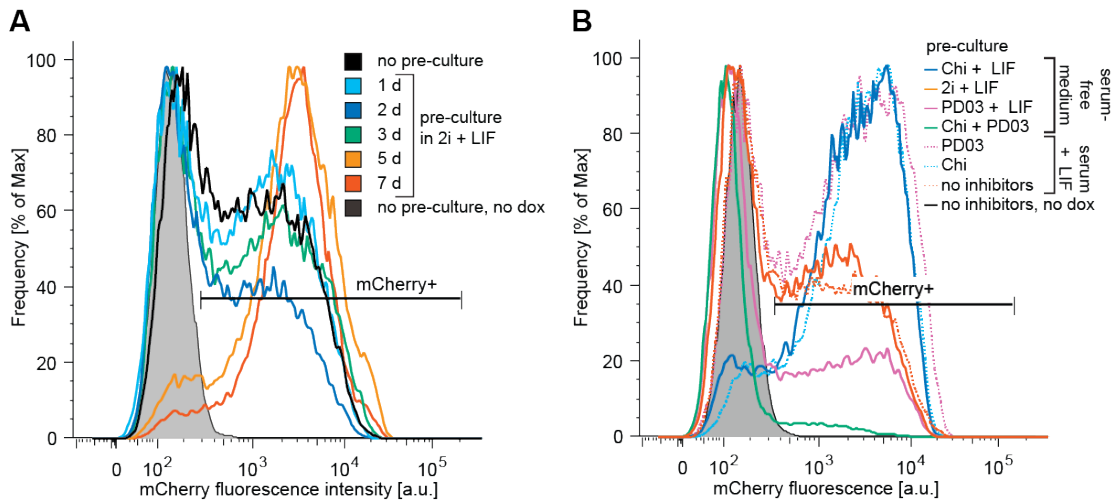


Fig. S4: Pre-culture regimes and –times affect the expression efficiency of the doxycycline-inducible transgene.

Cells grown for increasing periods of time in 2i + LIF medium (**A**) or cultured for 3 days in the indicated media (**B**) were changed to medium containing serum + LIF and doxycycline, followed by flow cytometric analysis for GATA4-mCherry expression 2 h after the end of a 6 h doxycycline pulse.

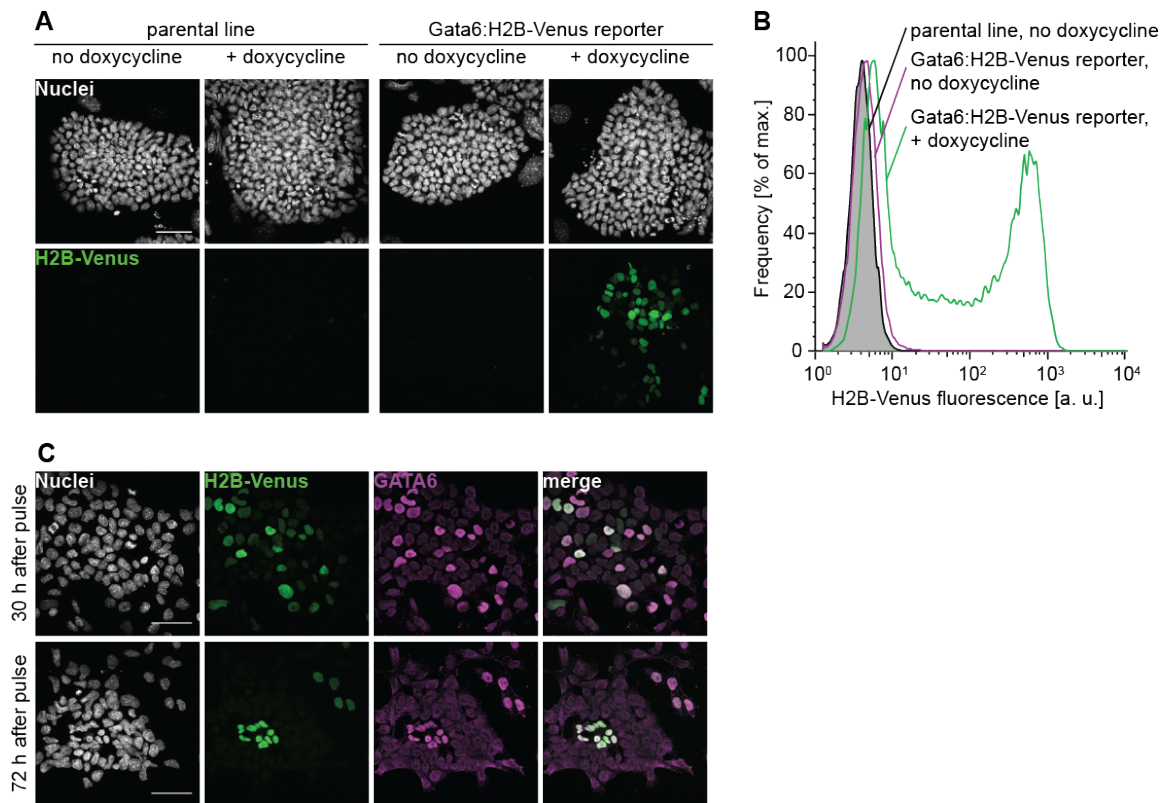


Fig. S5: The Gata6:H2B-Venus reporter is specifically expressed following doxycycline treatment, and recapitulates GATA6 protein expression over several days.

A Immunostaining for Venus expression in the parental cell line carrying the doxycycline-inducible GATA4-mCherry transgene (left) and the Gata6:H2B-Venus reporter cell line derived from it (right). Cells were either left untreated (left panels for each line), or treated with doxycycline for 6 h, followed by a 24 h chase period (right panel for each line). Scale bar, 50 μ m. **B** Flow cytometry of cells treated as in **A**. Venus expression can only be detected in reporter cells that have been treated with doxycycline. **C** Confocal microscopy of Gata6:H2B-Venus reporter cells immunostained for GATA6 protein 30 h (upper panels) or 72 h (lower panels) after a 6h doxycycline pulse. Correlation between GATA6 and reporter expression in individual cells increases for the 72 h time-point.

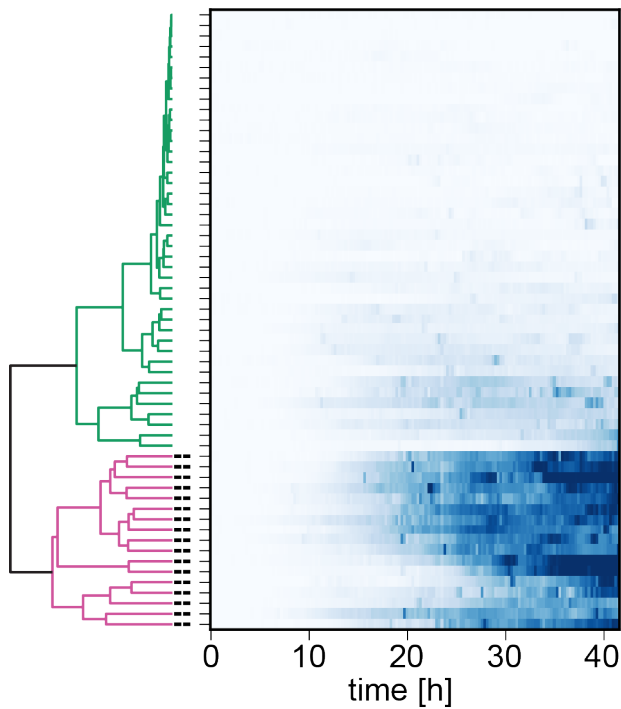


Fig. S6: Hierarchical clustering distinguishes groups of cells with high and low H2B-Venus expression in the Gata6 reporter line.

Gata6:H2B-Venus reporter cells were hierarchically clustered according to H2B-Venus fluorescence intensity values recorded during and after a 6 h doxycycline pulse. Dark blue indicates strong fluorescence. This analysis identifies two main groups that markedly differ in their H2B-Venus expression intensity in the second half of the experiment. These two groups are highlighted by different branch colors (green: H2B-Venus^{low}, purple: H2B-Venus^{high}), and inform the color code in Fig. 3G; see also supplementary material Movie 1.

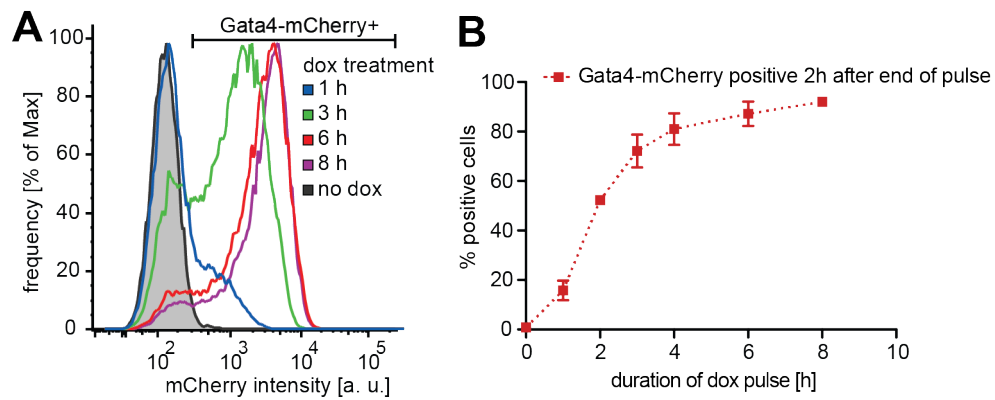


Fig. S7: Titration of GATA4-mCherry exposure by changing doxycycline pulse-length.

A Flow cytometric analysis of GATA4-mCherry expression in cells 2 h after the end of doxycycline pulses of indicated duration. **B** Quantification of results from **A**. Datapoints represent mean \pm standard deviation from three independent experiments.

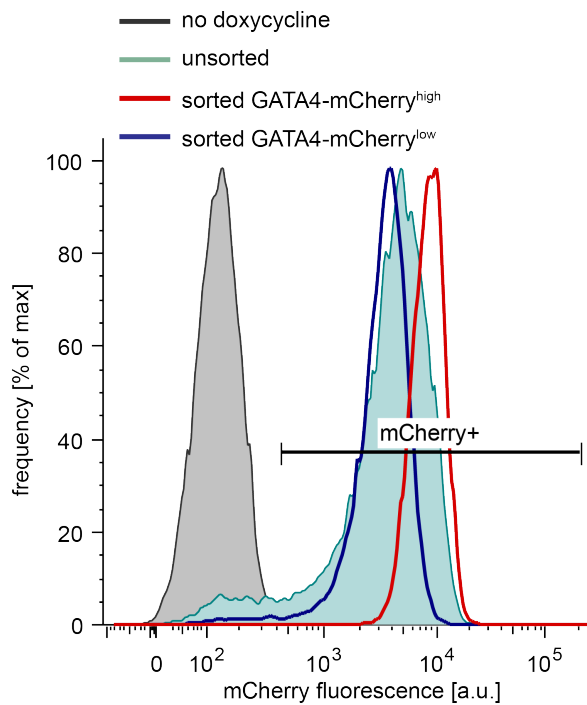


Fig. S8: Separation of GATA4-mCherry^{high} and GATA4-mCherry^{low} cells by flow cytometry.

Cells carrying a doxycycline-inducible GATA4-mCherry transgene were stimulated with doxycycline for 5 h, trypsinised and sorted into two fractions according to mCherry fluorescence intensity. Shows is the post-sort control, where fractions were analyzed on a separate cytometer approx. 2 h after the end of the sort for fluorescence levels and purity. The GATA4-mCherry^{high} population is in red, the GATA4-mCherry^{low} population is in blue, unsorted cells are in shaded in turquoise, and uninduced control is shaded in grey.

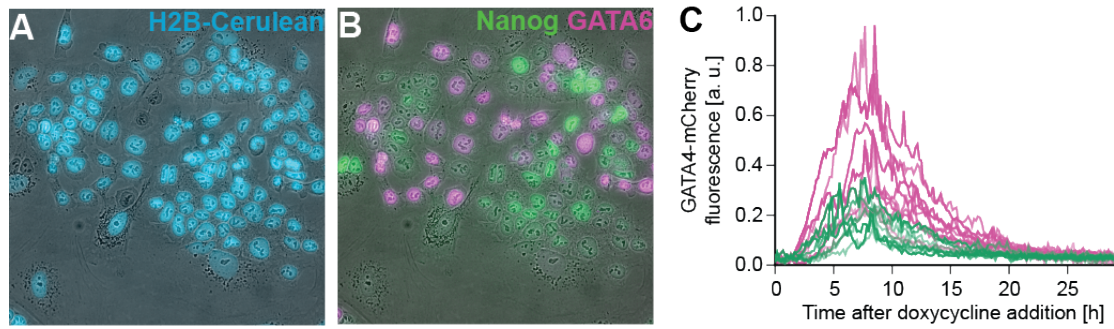


Fig. S9: Immunostaining of filmed cells for correlating GATA4-mCherry expression levels with fate choice.

A Overlay of brightfield and Cerulean fluorescence (blue) and **B** overlay of brightfield and immunostaining for Nanog (green) and GATA6 (purple) in cells carrying an inducible GATA4-mCherry transgene that had been filmed for 30 h during and after a doxycycline pulse. **C** Individual GATA4-mCherry fluorescence traces recorded from cells shown in supplementary material Movie 2 and panels **A**, **B**, color-coded according to staining detected in **B**. Cells without clear GATA6 or Nanog immunostaining are not shown in **C**.

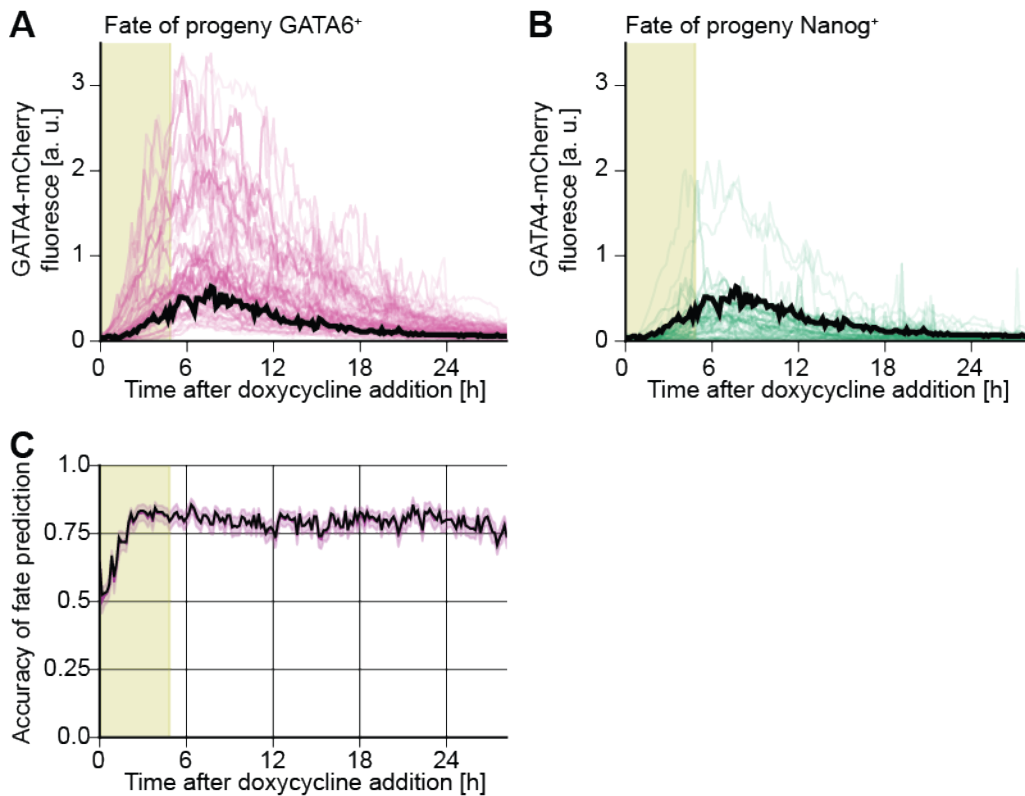


Fig. S10: Identification of an optimal threshold to predict fate choice from GATA4-mCherry expression levels.

A, B Fluorescence time traces of individual cells carrying an inducible GATA4-mCherry transgene filmed during and after a 6 h doxycycline pulse. Cells with GATA6-positive progeny are depicted with purple traces in **A**, cells with Nanog-positive progeny are depicted with green traces in **B**. The optimal threshold detected by ROC analysis (Fig. 4G) is shown in black. **C** Accuracy of fate prediction using GATA4-mCherry fluorescence and optimal threshold depicted in **A, B**. Fate choice can be predicted with greater than 80% accuracy approx. 3 h after addition of doxycycline. Area shaded in green indicates presence of doxycycline, area shaded in purple indicates standard deviation determined by bootstrapping.

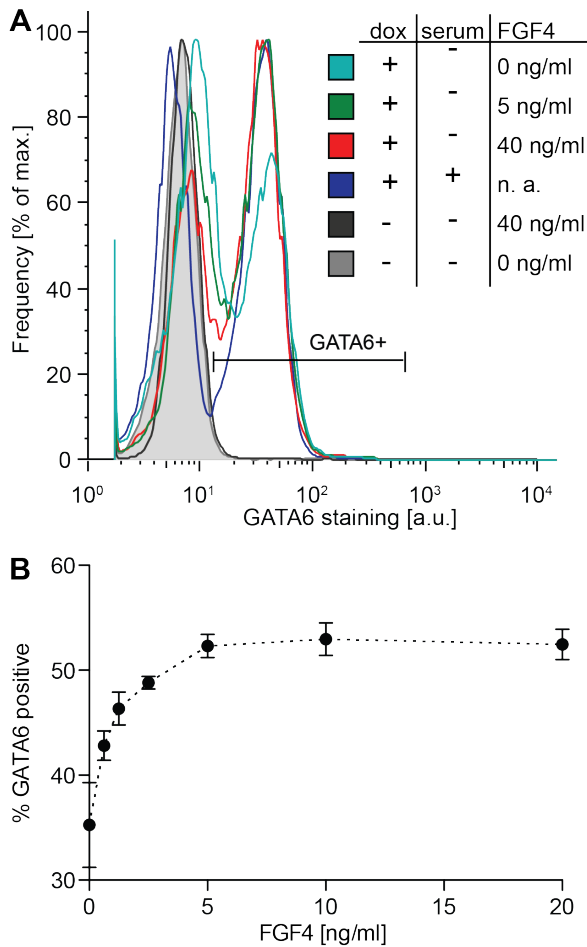


Fig. S11: Signaling in serum-free medium supports PrE-like differentiation

A Flow cytometry of cells stained for GATA6 that had been subjected to a 6 h doxycycline pulse and a 24 h chase period in the indicated media conditions. A large proportion of cells expresses GATA6 following doxycycline-treatment and differentiation in serum-free medium, and this proportion can only moderately be increased by addition of recombinant Fgf4. **B** Quantification of results from **A**. Data points show mean and standard error from two independent experiments. Note that the serum-free medium used in these experiments was supplemented with 1 μ g/ml heparin.

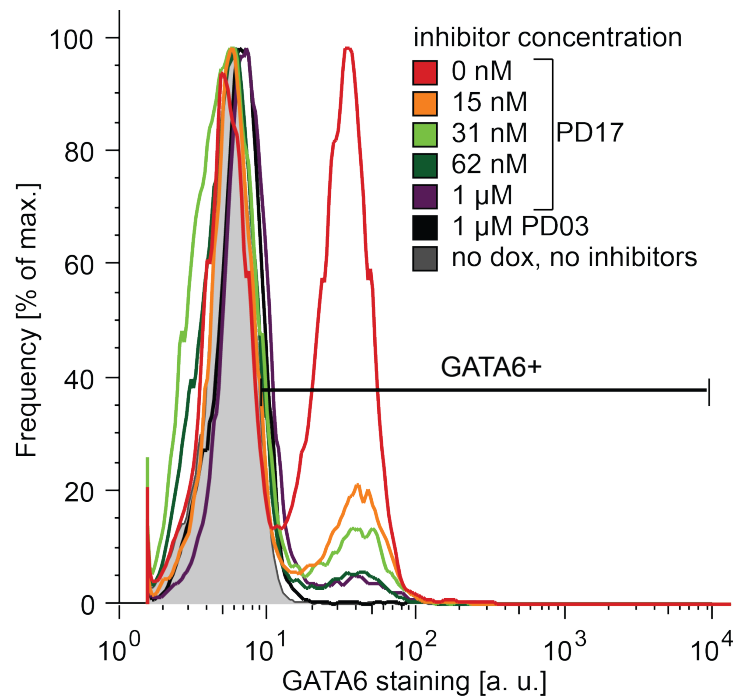


Fig. S12: MAPK signaling required for PrE-like differentiation is mainly triggered through FGF receptors.

Flow cytometric analysis of cells stained for GATA6 following a 6 h doxycycline pulse and a 24 h chase period in serum-containing medium with the indicated concentrations of the FGF receptor inhibitor PD17, or the Mek inhibitor PD03. PD17 inhibits most of PrE-like differentiation, indicating that the signaling input required for this differentiation decision is mainly transmitted through FGF receptors.

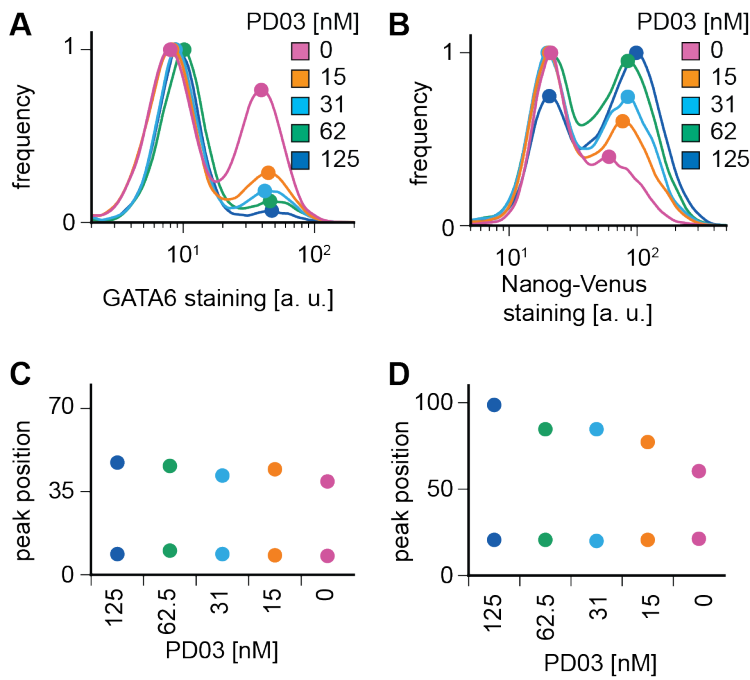


Fig. S13: Estimation of peak positions from flow cytometry data.

A, B Smoothened flow cytometry data from Fig. 5 C (GATA6 staining, **A**) and Fig. 7 C (Nanog-Venus staining, **B**) with peak positions indicated by dots. Histograms were smoothed by transforming each bin of the original data into a gaussian distribution of values around the center of the bin, and peaks were identified as local maxima in the smoothed distributions. **C, D** Peak positions identified in **A, B** plotted for different PD03 concentrations. The position of the peak with low staining levels comprising of GATA6-negative and Nanog-Venus-negative cells is constant for different PD03-concentrations, whereas the position of the Nanog-Venus-positive, but not the GATA6-positive peak, changes with signaling levels.

Supplementary Table

Table S1

Param.	Value	Units	Description
α_{N0}	$1^{a)}$ $1/2^{b)}$	<i>adimensional concentration</i> <i>units/h</i>	Maximum Nanog production rate in 0% signaling conditions. <i>a)</i> signaling inhibits Nanog production. <i>b)</i> signaling promotes GATA production.
α_{N1}	$1/2$	<i>adimensional concentration</i> <i>units/h</i>	Increase in the max. Nanog production rate in 100% signaling conditions.
α_{G0}	$1/2^{a)}$ $1/4^{b)}$	<i>adimensional concentration</i> <i>units/h</i>	Maximum endogenous Gata production rate in 0% signaling conditions. <i>a)</i> signaling inhibits Nanog production. <i>b)</i> signaling promotes GATA production.
α_{G1}	$1/2$	<i>adimensional concentration</i> <i>units/h</i>	Maximum endogenous Gata production rate in 100% signaling conditions.
λ_N	0.15	1/h	Nanog protein degradation rate.
λ_G	0.15	1/h	Gata protein degradation rate.
p	4	-	Hill coefficient for the inhibition of Nanog by Gata.
q	4	-	Hill coefficient for the inhibition of Gata by Nanog.
σ_D	0.25	<i>adimensional concentration</i> <i>units/h</i>	Scale parameter of the lognormal distribution of the maximum production rate of exogenous Gata in the presence of doxycycline.
τ	6	h	Doxycycline pulse duration

Table S1. Parameter values of the model.

Supplementary Experimental Procedures

Generation of engineered ES cell lines

Inducible transgenes were integrated into the KH2 cell line as described (Beard et al., 2006). The Gata6 reporter cell line was generated using knock-out first targeting arms of the EUCOMM project (Skarnes et al., 2011), combined with a H2B-Venus reporter cassette and a neomycin resistance gene driven from a human β -actin promoter. The targeting construct to generate the Nanog-Venus translational fusion has been described previously (Filipczyk et al., 2013). The construct used for permanent expression of the H2B-Cerulean marker was generated from pCX::H2B-mCherry described in (Nowotschin et al., 2009) by replacing the mCherry coding sequence with a Cerulean coding sequence. To generate reporter lines, approx. 2×10^6 cells were electroporated with 2 μ g of the linearized targeting vector, plated onto feeder cells and put under selection one day after electroporation. Resistant colonies were picked after seven days, and PCR-genotyped for correct insertion events (reporter constructs) or visually screened for transgene expression. Karyotypes of all genetically modified clones were determined according to standard procedures (Nagy et al., 2008), and clones with a median chromosome count of 40 were selected for experiments. Two subclones of the cell line carrying the inducible Gata4-mCherry construct gave high-contribution chimaeras with germline transmission, confirming that the ES cells used here retain full developmental potential.

Image processing and analysis

To quantify immunofluorescence intensity in single fixed cells, images were segmented based on nuclear fluorescence using methods available in FIJI (Schindelin

et al., 2012), and mean fluorescence intensities for individual channels measured in segmented regions after manual curation.

Spatial heterogeneities in fluorescence intensity in time-lapse recordings resulting from uneven illumination across the field of view were removed by taking 50 flatfield images without any cells, and normalizing fluorescence intensities from experimental movies with the average of the flatfield images. Temporal heterogeneities in fluorescence signal in the movies due to varying illumination intensities and medium autofluorescence were removed by measuring fluorescence intensity for at least three cell-free positions per movie, and subtracting their average fluorescence values from all measured pixel intensities. For some experiments, cells were fixed and immunostained for marker gene expression and returned to the microscope for imaging. Cells were tracked manually using the MTrackJ plugin of ImageJ (Erik Meijering, 2012), and fluorescence intensities in a region of interest around the trackpoint were extracted with custom-written Python scripts.

Receiver operating characteristics analysis

To compute receiver operating characteristics, we used a varying threshold level of GATA4-mCherry expression to make predictions based on the assumption that all cells above the threshold will differentiate, and those below it will not. These predictions were then compared to the real outcome, and for each threshold level we determined the ratio of correct and false predictions to the overall number of events (true positive ratio TPR, and false positive ratio, FPR). Plotting FPR versus TPR for all threshold values gives a characteristic curve for a single time-point (see Fig. 4G for an example). The area under this curve (AUC) is a measure of the ability of a classifier to predict an outcome – classifiers without predictive value have an AUC of

0.5, while a perfect predictor gives an AUC of 1.0. The ROC curve also allows determining the optimal threshold; in our case we used the threshold value that maximized the difference between TPR and FPR (red dot in Fig. 4G).

Mathematical modeling

The mathematical model proposed is based on the well studied mutual repression circuit (Gardner et al., 2000) and describes the dynamics of endogenous Gata (G) and Nanog (N) expression driven by externally induced Gata expression (G_X) with three rate equations (see results). The transient exogenous Gata G_X transcription rate was modeled with a rectangular step function π_τ of duration $\tau=6$ h. To account for the experimentally observed heterogeneity in the response to doxycycline, the maximum transcription rate parameter of G_X , D , was varied from cell to cell according to a log-normal distribution with scale parameter σ_D . Even though the experimentally observed distribution of GATA4-mCherry expression levels has a more complex distribution (Supplementary Fig. S7), we chose this simple, positively defined distribution to test generic dynamic behavior of the system following a range of GATA4-mCherry inputs. Gata and Nanog mutually repress each other's expression and this was accounted for by inhibitory Hill functions with cooperativity coefficients p and q . Exogenous Gata also participates in the repression of Nanog. For a given level of signaling, the maximal Gata and Nanog production rates α_G and α_N , which are attained in absence of their respective repressor, were assumed constant.

Regarding the interaction of signaling with this transcription network, we have considered two scenarios. In the first one we assumed that the maximum transcription rate for Nanog decreases linearly with the signal level s , $a_N(s) = a_{NI} s + a_{N0} (1-s)$, where $a_{NI} \leq a_{N0}$ while the maximum Gata transcription rate is not affected. The

second scenario we considered is a linear increase of the maximum Gata transcription rate with signal level, $a_G(s) = a_{G1} s + a_{G0} (1-s)$, $a_{G0} \leq a_{G1}$, and a constant Nanog transcription rate. In both cases signaling was assumed to be constant and equal in all cells. The model expresses concentrations normalized to the half-maximum inhibition concentration of the Hill functions, i.e., in arbitrary adimensional units. Time is expressed in dimensional units. Fitting exponential decay curves to normalized GATA4-mCherry fluorescence traces following the removal of doxycycline indicated a half-life of approx. 4 h for GATA4-mCherry, motivating us to set the decay rate λ_G for both exogenous and endogenous GATA factors to 0.15h^{-1} . We chose the same value for the Nanog protein decay rate λ_N , consistent with half-lives reported in the literature (Abranches et al., 2013; Muñoz-Descalzo et al., 2013). Thus, all but four parameter values of this system were constrained by experimental data (see Table S1 for all parameters used for simulations). Sensitivity analysis indicated that all parameter values could be changed at least two-fold without affecting the bistable behavior of the system. To reflect the pre-culturing of cells in the presence of PD03 we chose as initial condition for Nanog expression levels its steady state levels in the absence of signaling. Initial endogenous GATA levels were set to zero, reflecting the absence of detectable GATA expression in our ES cells in the absence of doxycycline stimulation. The visual representations of the potential landscape in Fig. 7E, F correspond to the path-integral quasi-potential surfaces as proposed by (Bhattacharya et al., 2011). These have been computed assuming no external supply of GATA factors.

Supplementary References

- Abranches, E., Bekman, E. and Henrique, D.** (2013). Generation and Characterization of a Novel Mouse Embryonic Stem Cell Line with a Dynamic Reporter of Nanog Expression. *PLoS ONE* **8**, e59928.
- Beard, C., Hochedlinger, K., Plath, K., Wutz, A. and Jaenisch, R.** (2006). Efficient method to generate single-copy transgenic mice by site-specific integration in embryonic stem cells. *Genesis* **44**, 23–28.
- Bhattacharya, S., Zhang, Q. and Andersen, M. E.** (2011). A deterministic map of Waddington's epigenetic landscape for cell fate specification. *BMC Syst Biol* **5**, 85.
- Erik Meijering, O. D. I. S.** (2012). Methods for Cell and Particle Tracking. 1–16.
- Filipczyk, A., Gkatzis, K., Fu, J., Hoppe, P. S., Lickert, H., Anastassiadis, K. and Schroeder, T.** (2013). Biallelic expression of nanog protein in mouse embryonic stem cells. *Cell Stem Cell* **13**, 12–13.
- Gardner, T. S., Cantor, C. R. and Collins, J. J.** (2000). Construction of a genetic toggle switch in *Escherichia coli*. *Nature* **403**, 339–342.
- Muñoz-Descalzo, S., Rué, P., Faunes, F., Hayward, P., Jakt, L. M., Balayo, T., Garcia-Ojalvo, J. and Martinez Arias, A.** (2013). A competitive protein interaction network buffers Oct4-mediated differentiation to promote pluripotency in embryonic stem cells. *Mol Syst Biol* **9**, 694.
- Nagy, A., Gertsenstein, M., Vintersten, K. and Behringer, R.** (2008). Karyotyping Mouse Cells. *Cold Spring Harbor ...*
- Nowotschin, S., Eakin, G. S. and Hadjantonakis, A.-K.** (2009). Dual transgene strategy for live visualization of chromatin and plasma membrane dynamics in murine embryonic stem cells and embryonic tissues. *Genesis* **47**, 330–336.
- Schindelin, J., Arganda-Carreras, I., Frise, E., Kaynig, V., Longair, M., Pietzsch, T., Preibisch, S., Rueden, C., Saalfeld, S., Schmid, B., et al.** (2012). Fiji: an open-source platform for biological-image analysis. *Nat Methods* **9**, 676–682.
- Skarnes, W. C., Rosen, B., West, A. P., Koutsourakis, M., Bushell, W., Iyer, V., Mujica, A. O., Thomas, M., Harrow, J., Cox, T., et al.** (2011). A conditional knockout resource for the genome-wide study of mouse gene function. *Nature* **474**, 337–342.